Proceedings of the
2007 IEEE Intelligent Vehicles Symposium
Istanbul, Turkey, June 13-15, 2007

Radar-Vision Based Vehicle Recognition with Evolutionary Optimized and Boosted Features

Ulrich Kadow, Georg Schneider and Alejandro Vukotich
Audi AG, Entwicklung Assistenzsysteme, 85045 Ingolstadt, Germany
ulrich.kadow@gmail.com, {georg2.schneider,alejandro.vukotich}@audi.de

***Abstract*— We present a real-time monocular vehicle detection and recognition system for driver assistance based on the fusion of data from a radar and a video sensor. The radar data is used both for narrowing down the size of the search area for vehicle rears on the video image and for the distance measurement of the vehicles in front. Using the passive video sensor a radar object is verified and the width as well as the lateral position of the vehicle are determined.**

The contribution of this work is threefold: At first, we present and apply a methodology for developing a novel evolutionary optimized symmetry measure. Secondly, we demonstrate a vehicle detection and recognition algorithm consisting of two steps: hypothesis generation using a detector based on a set of Haar-like filters and an AdaBoost learning algorithm and hypothesis verification using an evolutionary optimized and biologically motivated vehicle recognition system. Finally, the performance of both the individual components and the complete vehicle detection and recognition system is evaluated by not only using classical confusion matrices but also giving information on the accuracy of the width and lateral position sensing.

Our experimental results demonstrate a robust and real-time system trained and tested on more than 30,000 images.

I. INTRODUCTION

Driver assistance systems account for many different preventive safety functions in modern automobiles. Two of the most promising sensors for accomplishing such functions are the radar and the video sensor. While the use of radar sensors is already quite common within the luxury vehicle class, the incorporation of video sensors is still a very vigorous area of current research. An interesting approach is the fusion of the radar and video data, since it can provide several advantages: in particular improved reliability through detections from two independent sensors and the combination of the very accurate distance measurement by the radar sensors with the good lateral position accuracy obtained from the video processing. In this work we will present a vehicle detection system, that uses the advantages of both sensors through sensor fusion in order to achieve a more robust detection while compensating for limitations of each individual sensor. Generally, visual vehicle detection systems have high computational requirements as they need to process the acquired images at real-time. For the purpose of saving computation time in many cases two basic steps are used for the vehicle detection: 1) Hypothesis Generation (HG), in which the locations of possible vehicles in an image are hypothesized and 2) Hypothesis Verification (HV), in which tests are performed to verify the presence of vehicles on the found hypothesis [9].

There exist many different ways for performing the HG-step and in [9] the approaches are classified into three categories: 1) knowledge-based, 2) stereo-based, and 3) motion-based methods. Among the knowledge-based methods a quite common technique in the literature is to take advantage of the symmetric properties of vehicle rear views. In most cases, the hypothesized symmetry axis is used as a starting point for further processing. Following this approach once the symmetry axis has been found, in [8] the symmetric contours of the vehicle are followed out to their left- and rightmost bounds in order to determine the width of the detected object. In [18], a *symmetry enhancing edge detector* is developed based on a symmetry operator and used to identify the object contours. Through a search for strong vertical edges within the same distance to the hypothesized symmetry axis the vehicle borders are acquired in [1], [4], [2]. The work from Broggi et al. [5] uses edge symmetry for both determining the lateral vehicle position and for finding the vehicle's width through applying different sized search windows for the symmetry operator. Similar to [5] the work in [3] uses an edge symmetry detector for identifying the lateral vehicle position and its width while also exploiting information from the on-board radar sensors. In [15] the horizontal and vertical edge images are used to hypothesize a vehicle position, which is validated through a symmetry operator.

The step for the verification of the generated hypothesis (HV-step) can also be arranged through a big variety of possible methods. Again, an extensive review of template- and appearance-based methods can be found in [9]. It is hard to draw any conclusions by comparing the recognition results since all methods were tested on different sets of testing data. Nevertheless, considering only the test results on the respective test data, very good results for the recognition of vehicles in the HV-step could be achieved by using Haar wavelets and Gabor filters for generating features within the classification procedure. For instance, Haar wavelets have been used with much success in [10] and [11]. In [10], the detection rate approached 100% when the false positive rate was close to only 1 percent in the ROC curve. According to [9], the best results using Gabor filters was achieved within the work in [14], where a classification performed using support vector machines yielded an accuracy of 94.81%.

II. PROBLEM AND SETUP

For the purpose of detecting vehicles and determining their position, our experimental vehicle was equipped with a long range radar sensor behind the radiator grill and two short range radar sensors on the left and right front of the car. Furthermore, a monochrome video camera was installed behind the windshield close to the rear mirror.
The data from the radar sensors can be well exploited for the detection of vehicles in the video image by narrowing down the size and position of the search area in the video image. In order to compensate for the technically inherent longitudinal and lateral variance of the radar point in the video image, the search area for the vehicle detection in the video image has to be chosen quite generous as it has to be made sure that a full rear view of the vehicle to be detected is always included. With the radar point projected onto the image, we chose a total height of four meters and width of five meters (in the respective distance determined by the radar sensor) for the size of the search area. This 5x4 meter sized search area is then used for the HG-step of the video processing.
In order to fully understand the following sections, it is important to take a look at what data we used throughout our work. All training and testing data was generated from several recorded driving videos using the radar and video sensor described above. On each 5x4 meter sized search area on the whole video image around the radar reflex the exact position of the vehicles was marked by hand. In case there was a (negative) radar reflex (e.g. caused by the guardrail) a 2x2 meter sized box around the radar reflex was marked by hand. Additionally, one of the three class labels *CAR*, *TRUCK* and *NEGATIVE* was added to the marked position. All methods described in the following sections on the HG-step used the marked and labeled 5x4 meter sized images and all methods on the HV-step used the exactly cut out vehicle images derived from the marked position on the 5x4 meter sized image, respectively.

III. EVOLUTIONARY OPTIMIZED SYMMETRY

A. Symmetry Measures

A discrete one-dimensional image intensity function may be denoted by $f(x)$ (for the two-dimensional case the one-dimensional symmetry values for each line are just added up). Furthermore, let b denote the width of each line of the input image, which leads to a domain of $x \in [1,b]$. Let the variable $w \in \mathbb{N}$ with $w < \frac{1}{2}b$ denote the search window for the symmetry axis. The position of a symmetry axis may be defined by $x_s \in \mathbb{N}$ with $w < x_s \leq (b-w)$.

1) Gray-Level Symmetry without contrast normalization: The most intuitive and easiest way to calculate a symmetry measure for the given 1D intensity function $f(x)$ is just to subtract the symmetric intensity values and add up the results for all possible distances from the hypothesized symmetry axis. Hence, the value of x_s that belongs to the minimum of

$$S_g(x_s,w) = \sum_{x=1}^{w} |f(x_s-x) - f(x_s+x)| \tag{1}$$

would describe a possible location of a symmetry axis within $f(x)$.

2) Gray-Level Symmetry with contrast normalization: A drawback of the symmetry measure introduced above is its sensitivity with respect to different contrast conditions. That is, a dark object on a bright background would yield a much stronger extremum in equation (1) than a brighter one [17]. In [18] a symmetry measure is introduced that takes these observations into account as well. Let

$$G(x,x_s,w) = \begin{cases} \frac{1}{2}(f(x_s+x)+f(x_s-x)) & \text{,for } 1 \leq x \leq w \\ 0 & \text{,otherwise} \end{cases} \tag{2}$$

denote the even part of function $f(x)$ and

$$U(x,x_s,w) = \begin{cases} \frac{1}{2}(f(x_s+x)-f(x_s-x)) & \text{,for } 1 \leq x \leq w \\ 0 & \text{,otherwise} \end{cases} \tag{3}$$

denote the odd part, respectively. According to [18], with the normalized even function (normalized by subtracting the mean value)

$$G_n(x,x_s,w) = G(x,x_s,w) - \frac{1}{w}\sum_{x=1}^{w} G(x,x_s,w), \tag{4}$$

the complete symmetry measure for function $f(x)$ is defined by

$$S_{gc}(x_s,w) = \frac{\sum_{x=1}^{w} G_n(x,x_s,w)^2 - \sum_{x=1}^{w} U(x,x_s,w)^2}{\sum_{x=1}^{w} G_n(x,x_s,w)^2 + \sum_{x=1}^{w} U(x,x_s,w)^2}\ . \tag{5}$$

3) Edge Symmetry: Edge-based symmetry measures usually work on binarized edge images. In this paper edge-based symmetries using the binarized horizontal and vertical edge image as well as the binarized gradient image will be used. Since all symmetry measures using these input images are very similar, for simplicity reasons, edge symmetry will here only be formally introduced using the horizontal edge image. Let $E_h(x)$ be the binarized one-dimensional horizontal edge image generated from $f(x)$ using threshold θ_h. For calculating the horizontal edge symmetry measure we need a help function that determines, whether two pixels in the same distance from a given symmetry axis are symmetric:

$$S_e^p(x_s,d_w) = \begin{cases} 1 & \text{,if } E_h(x_s+d_w)=1 \text{ and } E_h(x_s-d_w)=1 \\ 0 & \text{,otherwise} \end{cases}, \tag{6}$$

where d_w denotes the distance from the position of the symmetry axis x_s. With S_e^p it is now possible to define an edge symmetry measure similar to [5] for the horizontal edge image through

$$S_e(x_s,w) = \frac{\left(\sum_{d_w=1}^{w} S_e^p(x_s,d_w)\right)^2}{\sum_{x_h=x_s-w}^{x_s+w} E_h(x_h)} \tag{7}$$

In words, the symmetry is computed as the ratio between the square of symmetric edges and all edges present in the considered search window.

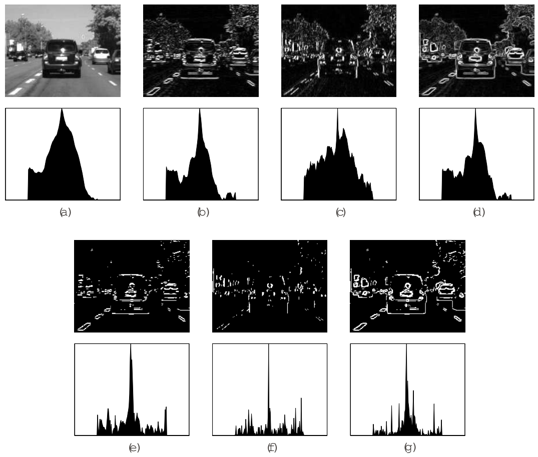

Fig. 1. The seven symmetry measures used in this work: (a) gray-level symmetry with contrast normalization; (b)-(d) gray-level symmetry without contrast normalization on the unthresholded horizontal, vertical and total gradient image; (e)-(g) edge symmetries on the binarized horizontal, vertical and total gradient image

B. Evolutionary Optimization

When taking into account that all (not only the edge symmetry) of the introduced symmetry measures above can be applied using different transformations of the original image function (e.g. the unthresholded gradient image), the question arises quickly, what symmetry measure in combination with what transformation works with the highest accuracy for our given task.

In order to achieve a more robust symmetry measure, in [2] gray-level symmetry as well as horizontal and vertical edge symmetry is added up to form a new combined symmetry measure called *total symmetry*. However, the question whether these three single symmetry measures are appropriate, whether and how each of these single measures should be weighted, and how the internal parametrization should be chosen (e.g. thresholds) remains unanswered.

In order to answer these questions in this work a total number of seven different symmetry measures are combined and several parameters of this combination are evolutionary optimized. Figure 1 shows all seven different symmetry measures. Note that no contrast normalization is used on the input images in figures 1b-d, since regions with intense contrast stand for strong edges and this should be emphasized by the symmetry operator.

Additionally, for each of these seven symmetry operators, the results of each line symmetry is weighted. Even though it is possible that the transformation of radar coordinates into image coordinates is not always correct due to external factors like the vehicle pitch, it is very likely that the vehicles are always within a certain sub-frame of the input image. In order to investigate this assumption, we assessed how often each line of the 5x4 meter sized sub-image actually contains a part of the vehicle rear and used the resulting distribution for our weighing process.

For simplicity, the seven symmetry operators described above will be henceforth denoted by S_1 through S_7. The final combined symmetry measure S_{opt} is the weighted sum of S_1 through S_7 and thus the position of the symmetry axis $\widehat{x_s}$ using that operator can be defined by

$$\widehat{x_s} = \mathrm{pos}_{max}\left(S_{opt}(x_s, w)\right) = \mathrm{pos}_{max}\left(\sum_{i=1}^{7} c_i S_i(x_s, w)\right) \quad (8)$$

where the function pos_{max} denotes the position of the maximum value and the $c_1, \ldots, c_7$ are the weights for each symmetry measure ($\forall\, c_i,\ i \in \{1, \ldots, 7\} : 0 \leq c_i \leq 1$ and $\sum_{i=1}^{7} c_i = 1$). Additionally, the search window size w as well as appropriate thresholds for the binarized horizontal, vertical and total gradient images need to be chosen. Let these four variables be denoted by c_8 through c_{11}. Since all of our data is marked with the correct position of a symmetry axis with respect to the vehicle rear, it is possible to calculate the deviation of the calculated symmetry axis $\widehat{x_s}$ from the by hand labeled symmetry axis x_s^* for a given input image I:

$$d_{symm}(c_1, \ldots, c_{11}, I) = \mathrm{abs}(\widehat{x_s} - x_s^*) \quad (9)$$

With n_I labeled input images, it is desirable that

$$F(\mathbf{c}) = \frac{1}{n_I} \sum_{i=1}^{n_I} d_{symm}(\mathbf{c}, I_i)^2 \rightarrow \min \quad (10)$$

where $\mathbf{c} = (c_1, \ldots, c_{11})$. For instance, if $F(\mathbf{c}) = 0$, the combined symmetry measure S_{opt} would always return the exact symmetry axis of the vehicle rear as marked on all test images. In our work, we used (10) as the target function for an evolutionary optimization algorithm using evolution strategies. For a good introduction on such optimization procedures see [6].

IV. HYPOTHESIS GENERATION

Within the HG-step it is important that the hypothesized positions of vehicles are as exact as possible, since an inaccurate position (e.g. a cut-off vehicle) will directly reduce the classification performance of the following HV-step. On the contrary, it is allowed to hypothesize some non-vehicles (false positives), since these should be classified into the negative class in the next step. However, if the amount of false positives is too big, the computation time increases rapidly.

We found that many low level hypothesis generation methods like searches for specific edges and corners or solely symmetry considerations are too inaccurate and deliver too many hypothesized vehicle positions. In fact, when there are many objects and shadows present in the image, our studies have shown that such methods even loose their applicability, since the overall detection and recognition rate went below 45%.

For the purpose of hypothesis generation, we mainly follow the approach used in [16]. That is, image regions are described by their responses under a family of Haar-like filters which are sensitive for instance to the presence of horizontal and vertical bars. Using this description a learning algorithm, based on AdaBoost, is applied yielding extremely efficient

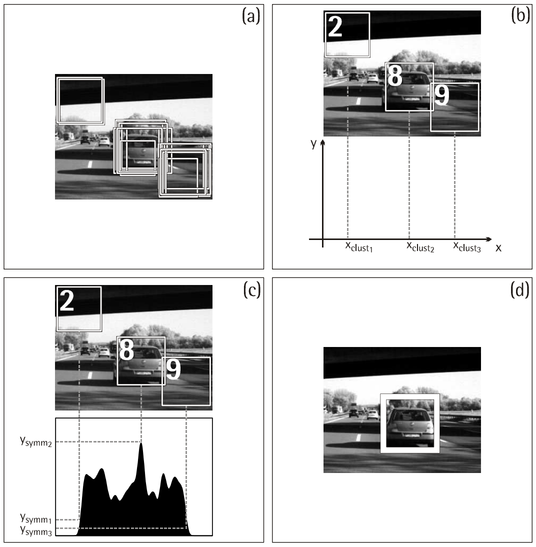

Fig. 2. The four steps of our HG-step: (a) finding all possible vehicle positions using a detector based on a set of Haar-like filters and an AdaBoost learning algorithm; (b) clustering of the results; (c) cluster-selection based on our evolutionary optimized symmetry measure; (d) final result

vehicle detectors. Thus, our HG-step already includes a fully functional vehicle detector with the nice property of very high detection rates, if the detector's parameter set allows some false positive detections.

In addition, we improved the performance by exploiting information from the optimized symmetry measure introduced in the previous section. In more detail, the full HG-step includes the following four subordinate processing steps.

The *first step* is to find all positions of vehicles, that might contain a possible candidate for the HG-step. The input to this processing is the 5x4 meter sized sub-image as described in section II. Furthermore, it is possible to exploit the additional information from the radar sensor. That is, we can look for only *reasonable* rectangles. Reasonable in this context means, that we can set a minimum width of the hypothesized rectangles to 1.5 meters (in the respective distance determined by the radar sensor). Figure 2a shows the result of our vehicle detector, which was developed using the learning algorithm, based on AdaBoost, as described in [16].

The result of the previous step yields many detections, especially at almost the same positions. Thus, the output of the previous step cannot be used as immediate result. Within our *second step*, we use a hierarchical clustering approach with an appropriate threshold in order to cluster the set of hypothesized vehicle positions. From each cluster subset we only take the average rectangle for the further processing. Figure 2b shows the resulting average rectangles. The numbers in the upper left corner depict the number of rectangles in the respective cluster.

The number of rectangles in a cluster is a good indicator of the detectors confidence and thus might be taken as decision rule for picking the right cluster as hypothesized vehicle position. However, this might not always result in a correct hypothesis. As in the example of figure 2b there are more rectangles in a wrong cluster due to effects (e.g. shadows) that interfere with the detection result. In order to solve this problem, we use the optimized symmetry operator S_{opt} within our *third processing step*. For that purpose the number of elements in each cluster is multiplied with the value of the symmetry operator at the respective position. The resulting highest score from this operation determines the target cluster. Figure 2c illustrates this processing.

Within our *fourth processing step*, the average rectangle of the target cluster from the previous step is considered as the final single hypothesis. The corresponding sub-image is cut out and passed on to the HV-step. Figure 2d shows the final cut out vehicle rear.

V. HYPOTHESIS VERIFICATION

In [12], [13] an object recognition system is presented, which solves the problem of object recognition using biological basic principals. In our work we used this recognition system for the HV-step. In essence, it is based on a transformation of the image objects into a high-dimensional feature space. Within this space, the classification is done by using a nearest neighbor classifier. The main characteristics of that approach are threefold. First, a fast processing with a high accuracy. Second, the image features for the recognition task are chosen by evolutionary optimization leading to an optimal set of features for the given task. Lastly, the recognition system is invariant towards small transitions of the object to be detected. That is, if the previous HG-step hypothesized a vehicle position with a slight offset, the recognition system is able to classify the sub-image correctly.

VI. RESULTS

First, all introduced single steps of our vehicle recognition system will be assessed one by one. That is, the optimized symmetry, the HG-step and the HV-step will be evaluated separately. Thereafter, the complete system using the HG- and HV-step together is evaluated. If reasonable, the used methods will be evaluated in regard to their correctness of the position sensing and the determination of the vehicle width.

A total of 1302 images including objects in a distance from 5 to 50 meters were labeled by hand into the classes *CAR* (380), *TRUCK* (105) , and *NEGATIVE* (817). For the purpose of simulating different rotations and displacements of the elements a vehicle rear contains (e.g. license plates, tail-lights, etc.) a total of 31248 images was generated using 23 different transformations including rotations, tilting, etc. Two thirds of that data was used for the training of the classifiers and the other third was used for all tests. Of course, the realization of this split took into account that there have to be no identical rear views of vehicles in either of the two sets.

A. Evolutionary Optimized Symmetry

Table I shows the results of all symmetry measures introduced in this paper. S_8 is the *total symmetry* measure, which was introduced in [2]. For the generation of the results of S_1 through S_8 the following parameters were used. The size of the search window w was set to one meter (in the respective distance determined by the radar sensor) and all thresholds for the generation of the binarized edge images were set to 30% of the maximum value in the gradient image. The column with caption d denotes the lateral deviation of the calculated symmetry axis from the marked symmetry axis. Caption s denotes the standard deviation of this lateral deviation. Both are given in pixels and centimeters.

Leaving the evolutionary optimized symmetry measure S_{opt} out of consideration, it can easily be seen that the *total symmetry* measure achieves the best results. Hence, it seems to be reasonable to combine different symmetry measures. Our developed symmetry measure S_{opt} reduced the deviation again by almost 50%! In the optimal setting of the eleven parameters $c_1, \ldots, c_{11}$ the weight values of the symmetry measures suggested that gray level symmetry with contrast normalization on the original input image, gray level symmetry without contrast normalization on the unthresholded horizontal gradient image as well as the edge symmetries on the horizontal and vertical edge images are most important. In addition it was noticeable that the threshold for the generation of the horizontal edge image was quite low. This leads to the conclusion, that all horizontal edges of vehicles, even the very weak ones, are significant for the symmetry calculation. This is consistent with the argumentation about the importance of horizontal edges for the detection of vehicles in [7].

B. HG-step

Even though our hypothesis generation depends on both the detection with Haar-like features and symmetry calculations, most of the quality depends on the performance of the former. The ROC-curve of our Haar-detector for the detection of vehicles of classes *CAR* and *TRUCK* showed a true-positive-rate of 97.4% at a corresponding false-negative rate of 2.6% and an average false-positive rate of 10%. In addition, the already high true-positive-rate descends from a quite strict criterion. If a found vehicle position deviates more than half a meter (in the respective distance determined by the radar sensor) from the correctly marked one, the vehicle

TABLE I

RESULTS FOR THE SYMMETRY MEASURES

symmetry measure	d [px]	s [px]	d [cm]	s [cm]
$S_1(x_s,w)$	9.7	13.0	46.9	63.4
$S_2(x_s,w)$	13.6	15.8	66.9	78.1
$S_3(x_s,w)$	14.9	12.7	73.3	62.9
$S_4(x_s,w)$	13.5	15.3	66.1	75.5
$S_5(x_s,w)$	9.9	12.7	48.0	62.2
$S_6(x_s,w)$	16.6	12.9	81.8	64.6
$S_7(x_s,w)$	10.7	12.6	52.2	61.8
$S_8(x_s,w)$	7.7	11.6	37.0	56.1
$S_{opt}(x_s,w)$	4.5	8.5	21.3	40.3

TABLE II

WIDTH AND LATERAL POSITION SENSING OF THE HG-STEP

	without symmetry			
	d [px]	s [px]	d [cm]	s [cm]
lateral	5.4	13.4	15.5	36.9
width	7.8	12.4	19.8	24.3
	with symmetry			
	d [px]	s [px]	d [cm]	s [cm]
lateral	4.6	12.7	12.6	29.2
width	7.7	12.3	19.1	22.5

TABLE III

CONFUSION MATRIX OF THE HV-STEP

		PREDICTED		
		NEGATIVE	CAR	TRUCK
ACTUAL	NEGATIVE	92.3	5.1	2.6
	CAR	4.2	94.2	1.6
	TRUCK	15.3	17.8	66.9

rear view is considered as not found. The average false-positive rate of 10% is not a problem, since most of the false-positives will be classified into the negative class in the following HV-step.

Table II shows the results for the width and lateral position sensing. The upper part of the table depicts the results without usage of symmetry and the lower part takes symmetry into account as described earlier. Clearly, when taking our evolutionary optimized symmetry measure into the HG-step, this has the biggest effect on the lateral position measurement. Even though the width measurement became better as well, the biggest improvement could be achieved at the lateral position measurement with an about 20% better position measurement.

C. HV-step

After the evolutionary optimization of the hierarchical object recognition system from [12], [13] the confusion matrix in table III shows the performance. With an accuracy of 94.2% for vehicles of the class *CAR* the classifier performance belongs to the top results achieved so far in the area of vehicle recognition (see [9] for a review). The accuracy for the *TRUCK* class is lower, which is probably the result of the following two reasons. First, the amount of training data we were able to use was not as big as it was for the class *CAR*. Second, the *TRUCK*-class possesses a huge variety of different rear views, which makes the classification task much more complex.

D. Complete Vehicle Detection and Classification System

The complete vehicle detection and recognition system incorporates both the hypothesis generation and hypothesis verification. This complete system will be evaluated by two tables. The first is the classical confusion matrix, shown in table IV. Obviously, the results are not as good as they were in the separate evaluation of the HV-step, since the input is

TABLE V
WIDTH AND LATERAL POSITION SENSING OF THE COMPLETE SYSTEM

			PREDICTED							
			CAR				TRUCK			
			d [px]	s [px]	d [cm]	s [cm]	d [px]	s [px]	d [cm]	s [cm]
ACTUAL	CAR	lateral	2.5	5.8	6.1	6.8	8.6	8.6	12.6	22.6
		width	5.9	9.1	13.4	10.6	14.9	13.7	15.3	10.7
	TRUCK	lateral	10.7	28.1	36.1	34.1	2.6	5.5	12.2	32.0
		width	15.1	19.2	58.1	47.4	5.1	5.5	20.5	18.5

TABLE IV
CONFUSION MATRIX OF THE COMPLETE SYSTEM

		PREDICTED		
		NEGATIVE	CAR	TRUCK
ACTUAL	NEGATIVE	80.2	15.1	4.7
	CAR	7.3	90.3	2.4
	TRUCK	27.4	19.5	53.3

not given by the perfectly cut out images of vehicle rears, but the ones delivered by the HG-step. Of course, if the HG is not able to hypothesize the position of a vehicle rear with enough accuracy, this will reduce the quality of the HV-step. Table V evaluates the width and lateral position sensing of the detected and recognized vehicles of the complete system. Here, the deviation of the calculated lateral position from the marked one lies between 6-12 centimeters. The correspondent deviations in pixels (2-3 px) is now in such a small range, that even when marking vehicles by hand it would be hard to tell a difference. The same applies to the results for the class *TRUCK*.

VII. CONCLUSION AND FUTURE WORK

The goal of this work was to detect vehicles and determine their position as well as their width using the combination of a radar and a video sensor. For that purpose we developed a new method of building a combined symmetry measure using evolutionary optimization, which was able to reduce the error rates on our test data by almost 50% compared to the *total symmetry*. In combination with the new developed symmetry measure, we built a complete vehicle detection and recognition system, which yielded an accuracy of 90.3% for the *CAR* class. The recognition system on exactly cut out images even had an accuracy of 94.2%.

For the future work the most important step would be the integration of a tracking procedure in order to save the computation time of the HV-step. Also, it could be valuable to include some results of the symmetry calculations into the classification routine as an extra feature. The same applies to the Haar-like features used in the HG-step.

REFERENCES

[1] A. Bensrhair, M. Bertozzi, A. Broggi, P. Miché, S. Mousset, and G. Toulminet. A Cooperative Approach to Vision-based Vehicle Detection. In *Procs. IEEE Intl. Conf. on Intelligent Transportation Systems 2001*, pages 209–214, Oakland, USA, August 2001.

[2] M. Bertozzi, A. Broggi, A. Fascioli, and S. Nichele. Stereo Vision-based Vehicle Detection. In *Procs. IEEE Intelligent Vehicles Symposium 2000*, pages 39–44, Detroit, USA, October 2000.

[3] L. Bombini, P. Cerri, P. Medici, and G. Alessandretti. Radar-vision fusion for vehicle detection. In *3rd International Workshop on Intelligent Transportation*, Hamburg, Germany, March 2006.

[4] A. Broggi, M. Bertozzi, A. Fascioli, C. Guarino Lo Bianco, and A. Piazzi. Visual Perception of Obstacles and Vehicles for Platooning. *IEEE Trans. on Intelligent Transportation Systems*, 1(3):164–176, September 2000.

[5] A. Broggi, P. Cerri, and P. C. Antonello. Multi-Resolution Vehicle Detection using Artificial Vision. In *Procs. IEEE Intelligent Vehicles Symposium*, pages 310–314, Parma, Italy, June 2004.

[6] M. Dianati, I. Song, and M. Treiber. An Introduction to Genetic Algorithms and Evolution Strategies. Technical report, University of Waterloo, July 2002.

[7] K. Kluge, T. Kanade, and H. Kuga. Car recognition for the CMU Navlab. *Vision and Navigation, The Carnegie Mellon Navlab*, pages 95–115, 1990.

[8] A. Kuehnle. Symmetry-based recognition of vehicle rears. *Pattern Recognition Letters*, 12:249–258, 1991.

[9] R. Miller, Z. Sun, and G. Bebis. On-road vehicle detection: A review. *IEEE Trans. Pattern Anal. Mach. Intell.*, 28(5):694–711, May 2006.

[10] C. Papageorgiou and T. Poggio. A trainable system for object detection. *International Journal of Computer Vision*, 38(1):15–33, 2000.

[11] D. Ponsa, A. López, F. Lumbreras, J. Serrat, and T. Graf. 3D Vehicle Sensor based on Monocular Vision. In *Proceedings of the 8th International IEEE Conference on Intelligent Transportations Systems*, Vienna, Austria, September 2005.

[12] G. Schneider. *Evolutionäre Optimierung eines biologisch motivierten visuellen Objekterkennungssystems*. PhD thesis, Universität Bielefeld, Oktober 2004.

[13] G. Schneider, H. Wersing, B. Sendhoff, and E. Körner. Evolutionary optimization of a hierarchical object recognition model. *IEEE Trans. Systems, Man, Cybernetics, Part B: Cybernetics*, 35(3):426–437, 2005.

[14] Z. Sun, G. Bebis, and R. Miller. On-road vehicle detection using gabor filters and support vector machines. In *International Conference on Digital Signal Processing*, Greece, July 2002.

[15] F. Thomanek and D. Dickmanns. Obstacle Detection, Tracking and State Estimation for Autonomous Road Vehicle Guidance. In *Procs. of the 1992 IEEE/RSJ Intl. Conf. on Intelligent Robots and Systems*, pages 1399–1406, Raleigh, NC, July 1992.

[16] P. Viola and M. Jones. Rapid Object Detection using a Boosted Cascade of Simple Features. In *Accepted Conference on Computer Vision and Pattern Recognition*, 2001.

[17] M. Warnecke. Validierung von Umfeldmodellen anhand von Videosensorik. Master's thesis, University of Applied Sciences Wolfenbüttel, Germany, August 2002.

[18] T. Zielke, M. Brauckmann, and W. von Seelen. Intensity and Edge-Based Symmetry Detection with an Application to Car-Following. *CVGIP: Image Understanding*, 58(2):177–190, 1993.